

Assessment of N95 respirator decontamination and re-use for SARS-CoV-2

Robert J. Fischer¹, Dylan H. Morris², Neeltje van Doremalen¹, Shanda Sarchette¹, M. Jeremiah Matson¹
Trenton Bushmaker¹, Claude Kwe Yinda¹, Stephanie N. Seifert¹, Amandine Gamble³, Brandi N.
Williamson¹, Seth D. Judson⁴, Emmie de Wit¹, James O. Lloyd-Smith³, Vincent J. Munster¹

1. National Institute of Allergy and Infectious Diseases, Hamilton, MT
2. Princeton University, Princeton, NJ
3. University of California, Los Angeles, Los Angeles, CA
4. University of Washington, Seattle, WA

The unprecedented pandemic of COVID-19 has created worldwide shortages of personal protective equipment, in particular respiratory protection such as N95 respirators¹. SARS-CoV-2 transmission is frequently occurring in hospital settings, with numerous reported cases of nosocomial transmission highlighting the vulnerability of healthcare workers²⁻⁴. In general, N95 respirators are designed for single use prior to disposal. Several groups have addressed the potential for re-use of N95 respirators from a mechanical or from a decontamination perspective (for a full literature overview see Supplementary Appendix).

Here, we analyzed four different decontamination methods – UV radiation (260 – 285 nm), 70°C heat, 70% ethanol and vaporized hydrogen peroxide (VHP) – for their ability to reduce contamination with infectious SARS-CoV-2 and their effect on N95 respirator function. For each of the decontamination methods, we compared the inactivation rate of SARS-CoV-2 on N95 filter fabric to that on stainless steel, and we used quantitative fit testing to measure the filtration performance of the N95 respirators after each decontamination run and 2 hours of wear, for three consecutive decontamination and wear sessions (see Appendix). Vaporized hydrogen peroxide and ethanol yielded extremely rapid inactivation both on N95 and on stainless steel (Figure 1A). UV inactivated SARS-CoV-2 rapidly from steel but more slowly on N95 fabric, likely due its porous nature. Heat caused more rapid inactivation on N95 than on steel; inactivation rates on N95 were comparable to UV.

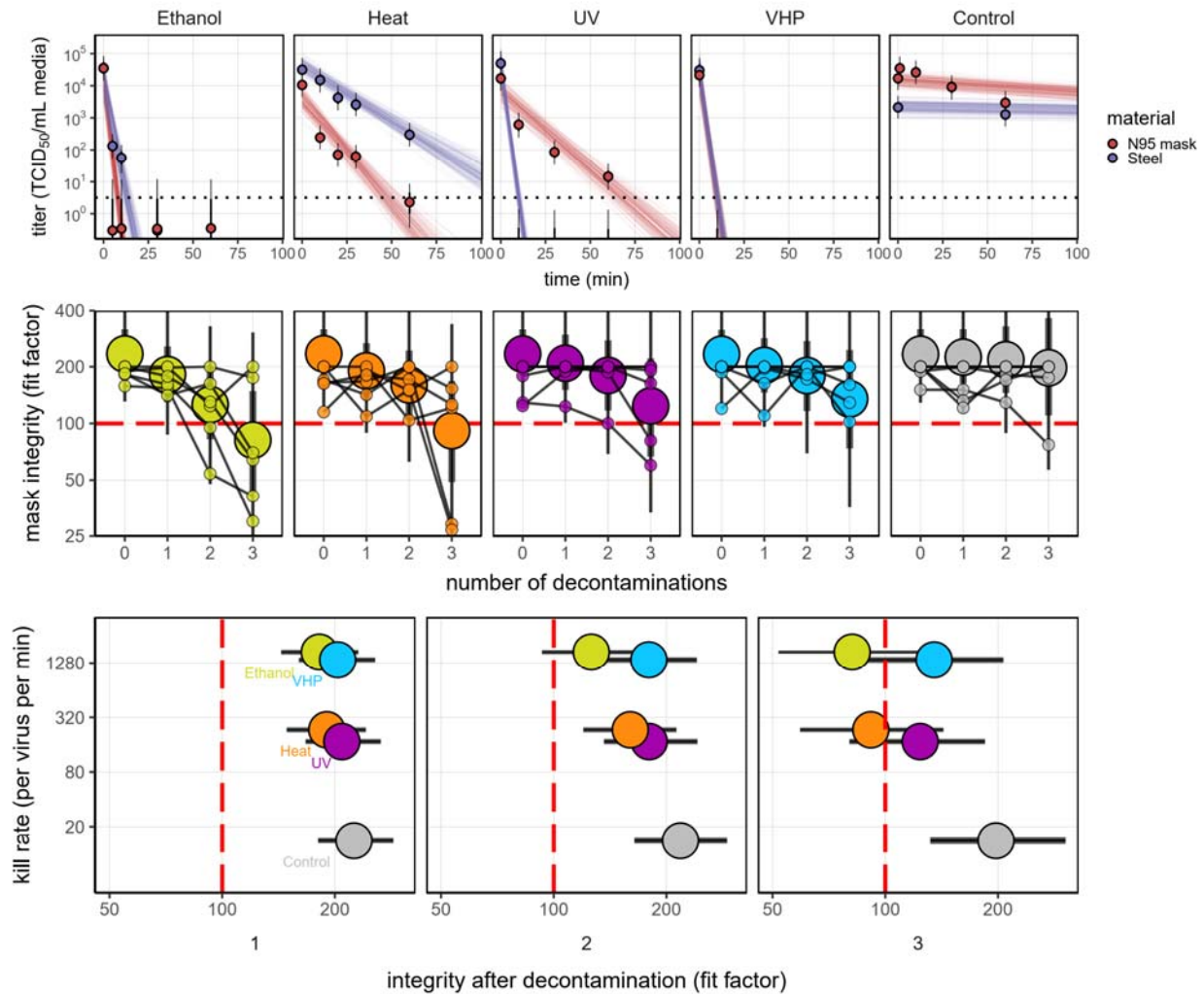
Quantitative fit tests showed that the filtration performance of the N95 respirator was not markedly reduced after a single decontamination for any of the four decontamination methods (Figure 1B). Subsequent rounds of decontamination caused sharp drops in filtration performance of the ethanol-treated masks, and to a slightly lesser degree, the heat-treated masks. The VHP- and UV-treated masks retained comparable filtration performance to the control group after two rounds of decontamination, and maintained acceptable performance after three rounds.

Taken together, our findings show that VHP treatment exhibits the best combination of rapid inactivation of SARS-CoV-2 and preservation of N95 respirator integrity, under the experimental conditions used here (Figure 1C). UV radiation kills the virus more slowly and preserves comparable respirator function. 70°C dry heat kills with similar speed and is likely to maintain acceptable fit scores for two rounds of decontamination. Ethanol decontamination is not recommended due to loss of N95 integrity, echoing earlier findings⁵.

All treatments, particularly UV and dry heat, should be conducted for long enough to ensure that a sufficient reduction in virus concentration has been achieved. The degree of required reduction will depend upon the degree of initial virus contamination. Policymakers can use our estimated decay rates together with estimates of degree of real-world contamination to choose appropriate treatment durations (see Appendix).

Our results indicate that N95 respirators can be decontaminated and re-used in times of shortage for up to three times for UV and HPV, and up to two times for dry heat. However, utmost care should be given to ensure the proper functioning of the N95 respirator after each decontamination using readily available qualitative fit testing tools and to ensure that treatments are carried out for sufficient time to achieve desired risk-reduction.

54



55

56 **Figure 1.** Decontamination of SARS-CoV-2 by four different methods. **A)** SARS-CoV-2 on N95 fabric

57 and stainless steel surface was exposed to UV, 70 °C dry heat, 70% ethanol and vaporized hydrogen

58 peroxide (VHP). 50 µl of 10⁵ TCID₅₀/mL of SARS-CoV was applied on N95 and stainless steel (SS).

59 Samples were collected at indicted timepoints post exposure to the decontamination method for UV, heat

60 and ethanol and after 10 minutes for VHP. Viable virus titer is shown in TCID₅₀/mL media on a

61 logarithmic scale. All samples were quantified by end-point titration on Vero E6 cells. Plots show

62 estimated mean across three replicates (dots and bars show the posterior median estimate of this mean and

63 the posterior inter-quartile range, or IQR). Lines show predicted decay of virus titer over time (lines; 50

64 random draws per replicate from the joint posterior distribution of the exponential decay rate, i.e. negative

of the slope, and intercept, i.e. initial virus titer). Black dashed line shows maximum likelihood estimate titer at the Limit of Detection (LOD) of the assay: $10^{0.5}$ TCID₅₀/mL media. **B)** Mask integrity. Quantitative fit testing results for all the decontamination methods after decontamination and 2 hours of wear, for three consecutive runs. Data from six individual replicates (small dots) for each treatment are shown in addition to the predicted median and IQR (large dots and bars respectively) fit factor. Fit factors are a measure of filtration performance: the ratio of the concentration of particles outside the mask to the concentration inside. The measurement machine reports value up to 200. A minimal fit factor of 100 (red dashed line) is required for a mask to pass a fit test. **C)** SARS-CoV-2 decontamination performance. Kill rate (y-axis), versus mask integrity after decontamination (x-axis; bar length represents IQR). The three panels report mask integrity after one, two or three decontamination cycles.

References

1. Health C for D and R. N95 Respirators and Surgical Masks (Face Masks). FDA [Internet] 2020 [cited 2020 Apr 10]; Available from: <https://www.fda.gov/medical-devices/personal-protective-equipment-infection-control/n95-respirators-and-surgical-masks-face-masks>
2. McMichael TM, Currie DW, Clark S, et al. Epidemiology of Covid-19 in a Long-Term Care Facility in King County, Washington. *New England Journal of Medicine* 2020; in press.
3. Wu Z, McGoogan JM. Characteristics of and Important Lessons From the Coronavirus Disease 2019 (COVID-19) Outbreak in China: Summary of a Report of 72 314 Cases From the Chinese Center for Disease Control and Prevention. *JAMA* 2020;323(13):1239–42.
4. Livingston E, Bucher K. Coronavirus Disease 2019 (COVID-19) in Italy. *JAMA* [Internet] 2020 [cited 2020 Apr 10]; Available from: <https://jamanetwork.com/journals/jama/fullarticle/2763401>
5. Liao L, Xiao W, Yu X, Wang H, Zhao M, Wang Q. Can N95 facial masks be used after disinfection? And for how many times? [Internet]. Stanford University and 4C Air, Inc; 2020 [cited 2020 Apr 10]. Available from: <https://stanfordmedicine.app.box.com/v/covid19-PPE-1-2>

95	Table of contents:	page 1
96	Supplemental methods	page 2
97	Supplemental table	page 9
98	Supplemental references	page 9
99	Code and data availability	page 10
100	Acknowledgements	page 10

Supplemental methods

Short literature review:

The COVID-19 pandemic has highlighted the necessity for large-scale decontamination procedures for PPE, in particular N95 respirator masks¹. SARS-CoV-2 has frequently been detected on PPE of healthcare workers². The environmental stability of SARS-CoV-2 underscores the need for rapid and effective decontamination methods³. Extensive literature is available for decontamination procedures for N95 respirators, using either bacterial spore inactivation tests, bacteria or respiratory viruses (e.g. influenza A virus)⁴⁻¹¹. Effective inactivation methods for these pathogens and surrogates include UV, ethylene oxide, vaporized hydrogen peroxide, gamma irradiation, ozone and dry heat^{4,6,8,10-13}. The filtration efficiency and N95 respirator fit has typically been less well explored, but suggest that both filtration efficiency and N95 respirator fit can be affected by the decontamination method used^{12,14}. It will therefore be critical that FDA, CDC and OSHA guidelines with regards to fit testing, seal check and respirator re-use are followed^{4,15-18}.

Laboratory experiments

Viruses and titration

HCoV-19 nCoV-WA1-2020 (MN985325.1) was the SARS-CoV-2 strain used in our comparison¹⁹. Virus was quantified by end-point titration on Vero E6 cells as described previously²⁰. Virus titrations were performed by end-point titration in Vero E6 cells. Cells were inoculated with 10-fold serial dilutions in four-fold of samples taken from N95 mask and stainless steel surfaces (see below). One hour after inoculation of cells, the inoculum was removed and replaced with 100 µl (virus titration) DMEM (Sigma-Aldrich) supplemented with 2% fetal bovine serum, 1 mM L-glutamine, 50 U/ml penicillin and 50 µg/ml streptomycin. Six days after inoculation, cytopathogenic effect was scored and the TCID₅₀ was calculated (see below). Wells presenting cytopathogenic effects due to media toxicity (e.g., due to the presence of ethanol or hydrogen peroxide) rather than viral infection were removed from the titer inference procedure.

N95 and stainless steel surface

N95 material discs were made by punching 9/16" (15 mm) fabric discs from N95 respirators, AOSafety N9504C respirators (Aearo Company Southbridge, MA). The stainless steel 304 alloy discs were purchased from Metal Remnants (<https://metalremnants.com/>) as described previously. 50 µL of SARS-CoV-2 was spotted onto each disc. A 0 time-point measurement was taken prior to exposing the discs to the disinfection treatment. At each sampling time-point, discs were rinsed 5 times by passing the medium over the stainless steel or through the N95 disc. The medium was transferred to a vial and frozen at -80°C until titration. All experimental conditions were performed in triplicate.

Decontamination methods

Ultraviolet light. Plates with fabric and steel discs were placed under an LED high power UV germicidal lamp (effective UV wavelength 260-285nm) without the titanium mesh plate (LEDi2, Houston, Tx) 50 cm from the UV source. At 50 cm the UVAB power was measured at 5 µW/cm² using a General UVAB digital light meter (General Tools and Instruments New York, NY). Plates were removed at 10, 30 and 60 minutes and 1 mL of cell culture medium added.

Heat treatment. Plates with fabric and steel discs were placed in a 70°C oven. Plates were removed at 10, 20, 30 and 60 minutes and 1 mL of cell culture medium added.

70% ethanol. Fabric and steel discs were placed into the wells of one 24 well plate per time-point and sprayed with 70% ethanol to saturation. The plate was tipped to near vertical and 5 passes of ethanol were sprayed onto the discs from approximately 10 cm. After 10 minutes,, 1 mL of cell culture medium was added.

Vaporized hydrogen peroxide (VHP). Plates with fabric and steel discs were placed into a Panasonic MCO-19AIC-PT (PHC Corp. of North America Wood Dale, IL) incubator with VHP generation capabilities and exposed to hydrogen peroxide (approximately 1000 ppm). The exposure to VHP was 10 minutes, after the inactivation of the hydrogen peroxide, the plate was removed and 1 mL of cell culture medium was added.

Control. Plates with fabric and steel discs and steel plates were maintained at 21-23°C and 40% relative humidity for up to four days. After the designated time-points, 1 mL of cell culture medium was added.

N95 mask integrity testing

N95 Mask (3M™ Aura™ Particulate Respirator 9211+/37193) integrity testing after 2 hours of wear and decontamination, for three consecutive rounds, was performed for a total of 6 times for each decontamination condition and control condition. Masks were worn by subjects and integrity was quantitatively determined using the Portacount Respirator fit tester (TSI, 8038) with the N95 companion component, following the modified ambient aerosol condensation nuclei counter quantitative fit test protocol approved by the OSHA (Occupational Safety and Health Administration, 2012). Subjects were asked to bend over for 40 seconds, talk for 50 seconds, move head from side-to-side for 50 seconds, and move head up-and-down for 50 seconds whilst aerosols on inside and outside of mask were measured. By convention, this fit test is passed when the final score is ≥ 100 . For the N95 integrity testing, a Honeywell Mistmate humidifier (cat#HUL520B) was used for particle generation.

Statistical analyses

In the model notation that follows, the symbol \sim denotes that a random variable is distributed according to the given distribution. Normal distributions are parametrized as Normal(mean, standard deviation). Positive-constrained normal distributions (“Half-Normal”) are parametrized as Half-Normal(mode, standard deviation). Normal distributions truncated to the interval $[0, 1]$ are parameterized as TruncNormal(mode, standard deviation).

We use $\langle \text{Distribution Name} \rangle \text{CDF}(x \mid \text{parameters})$ and $\langle \text{Distribution Name} \rangle \text{CCDF}$ to denote the cumulative distribution function and complementary cumulative distribution functions of a probability distribution, respectively. So for example NormalCDF(5 | 0, 1) is the value of the Normal(0, 1) cumulative distribution function at 5.

We use $\text{logit}(x)$ and $\text{invlogit}(x)$ to denote the logit and inverse logit functions, respectively:

$$\text{logit}(x) = \ln \frac{x}{1-x} \quad (1)$$

$$\text{invlogit}(x) = \frac{e^x}{1 + e^x} \quad (2)$$

Mean titer inference

We inferred mean titers across sets of replicates using a Bayesian model. The \log_{10} titers v_{ijk} (the titer for the sample from replicate k of timepoint j of experiment i) were assumed to be normally distributed about a mean μ_{ij} with a standard deviation σ . We placed a very weakly informative normal prior on \log_{10} titers μ_{ij} :

$$\mu_{ij} \sim \text{Normal}(3, 3) \quad (3)$$

We placed a weakly informative normal prior on the standard deviation:

$$\sigma \sim \text{Normal}(0, 0.5) \quad (4)$$

We then modeled individual positive and negative wells for sample ijk according to a Poisson single-hit model²¹. That is, the number of virions that successfully infect cells in a given well is Poisson distributed with mean:

$$V = \ln(2) 10^v \quad (5)$$

where v is the \log_{10} virus titer in TCID₅₀, where v is the \log_{10} virus titer in TCID₅₀, and the well is infected if at least one virion successfully infects a cell. The value of the mean derives from the fact that our units are TCID₅₀; the probability of infection at $v = 0$, i.e. 1 TCID₅₀, is equal to $1 - e^{-\ln(2) \times 1} = 0.5$.

Let Y_{ijkdl} be a binary variable indicating whether the l^{th} well of dilution factor d (expressed as \log_{10} dilution factor) of sample ijk was positive (so $Y_{ijkdl} = 1$ if the well was positive and 0 otherwise), which will occur as long as at least one virion successfully infects a cell.

It follows from (5) that the conditional probability of observing $Y_{ijkdl} = 1$ given a true underlying titer \log_{10} titer v_{ijk} is given by:

$$L(Y_{ijkdl} = 1 \mid v_{ijk}) = 1 - e^{-\ln(2) \times 10^x} \quad (6)$$

Where

$$x = v_{ijk} - d \quad (7)$$

is the expected concentration, measured in \log_{10} TCID₅₀, in the dilute sample. This is simply the probability that a Poisson random variable with mean $(-\ln(2) \times 10^x)$ is greater than 0. Similarly, the conditional probability of observing $Y_{ijkl} = 0$ given a true underlying titer \log_{10} titer v_{ijk} is given by:

$$L(Y_{ijkl} = 0 | v_{ijk}) = e^{-\ln(2) \times 10^x} \quad (8)$$

which is the probability that the Poisson random variable is 0.

This gives us our likelihood function, assuming independence of outcomes across wells.

Virus inactivation regression

The durations of detectability depend on the decontamination treatment but also initial inoculum and sampling method, as expected. We therefore estimated the decay rates of viable virus titers using a Bayesian regression analogous to that used in van Doremalen et al., 2020³. This modeling approach allowed us to account for differences in initial inoculum levels across replicates as well as other sources of experimental noise. The model yields estimates of posterior distributions of viral decay rates and half-lives in the various experimental conditions – that is, estimates of the range of plausible values for these parameters given our data, with an estimate of the overall uncertainty²².

Our data consist of 10 experimental conditions: 2 materials (N95 masks and stainless steel) by 5 treatments (no treatment, ethanol, heat, UV and VHP). Each has three replicates, and multiple time-points for each replicate. We analyze the two materials separately. For each, we denote by Y_{ijkl} the positive or negative status (see above) for well l which has dilution d for the titer v_{ijk} from experimental condition i during replicate j at time-point k .

We model each replicate j for experimental condition i as starting with some true initial \log_{10} titer $v_{ij}(0) = v_{ij0}$. We assume that viruses in experimental condition i decay exponentially at a rate λ_i over time t . It follows that:

$$v_{ij}(t) = v_{ij0} - \lambda_i t \quad (9)$$

We use the direct-from-well data likelihood function described above, except that now instead of estimating titer distribution about a shared mean μ_{ij} we estimate λ_i under the assumptions that our observed well data Y_{ijkl} reflect the titers $v_{ij}(t)$.

Regression prior distributions

We place a weakly informative Normal prior distribution on the initial \log_{10} titers v_{ij0} to rule out implausibly large or small values (e.g. in this case undetectable \log_{10} titers or \log_{10} titers much higher than the deposited concentration), while allowing the data to determine estimates within plausible ranges:

$$v_{ij0} \sim \text{Normal}(4.5, 2) \quad (10)$$

We placed a weakly informative Half-Normal prior on the exponential decay rates λ_i :

$$\lambda_i \sim \text{Half-Normal}(0.5, 4) \quad (11)$$

Our plated samples were of volume 0.1 mL, so inferred titers were incremented by 1 to convert to units of \log_{10} TCID₅₀/mL.

Mask integrity estimation

To quantify the decay of mask integrity after repeated decontamination, we used a logit-linear spline Bayesian regression to estimate the rate of degradation of mask fit factors over time, accounting for the fact that fit factors are interval-censored ratios. Fit factors are defined as the ratio of exterior concentration to interior concentration of a test aerosol. They are reported to the nearest integer, up to a maximum readout of 200, but arbitrarily large true fit factors are possible as the mask performance approaches perfect filtration.

We had 6 replicate masks j for each of 5 treatments i (no decontamination, ethanol, heat, UV and VHP). Each mask j was assessed for fit factor at 4 time-points k : before decontamination, and then after 1,

2, and 3 decontamination cycles. We label the control treatment $i = 0$. So we denote by F_{ijk} the fit factor for the j^{th} mask from the i^{th} treatment after k decontaminations (with $k = 0$ for the initial value).

We first converted fit factors F_{ijk} to the equivalent observed filtration rate Y_{ijk} by:

$$Y = 1 - 1/F \quad (12)$$

Observation model and likelihood function

We modeled the censored observation process as follows. $\text{logit}(Y_{ijk})$ values are observed with Gaussian error about the true filtration $\text{logit}(p_{ijk})$, with an unknown standard deviation σ_o , and then converted to fit factors, which are then censored:

$$\text{logit}(Y_{ijk}) \sim \text{Normal}(\text{logit}(p_{ijk}), \sigma_o) \quad (13)$$

Because our reported fit factors are known to be within integer values and right-censored at 200, for $F_{ijk} \geq 200$ we have a conditional probability of observing the data given the parameters of

$$L(F_{ijk} | p_{ijk}, \sigma_o) = \text{NormalCCDF}(\text{logit}(1 - 1/200) | \text{logit}(p_{ijk}) \sigma_o) \quad (14)$$

That is, we calculate the probability of observing a value of F greater than or equal to 200 (equivalent a value of Y greater than or equal to $1 - 1/200$), given our parameters.

For $1.5 \leq F_{ijk} < 200$, we first calculate the upper and lower bounds of our observation $Y_{ijk}^+ = 1 - 1 / (F_{ijk} - 0.5)$ and $Y_{ijk}^- = 1 - 1 / (F_{ijk} + 0.5)$. Then:

$$L(F_{ijk} | p_{ijk}, \sigma_o) = \text{NormalCDF}(\text{logit}(Y_{ijk}^+) | \text{logit}(p_{ijk}) \sigma_o) - \text{NormalCDF}(\text{logit}(Y_{ijk}^-) | \text{logit}(p_{ijk}) \sigma_o) \quad (15)$$

That is, we calculate the probability of observing a value between Y_{ijk}^+ and Y_{ijk}^- , given our parameters.

Decay model

We assumed that each mask had some true initial filtration rate p_{ij0} . We assumed that these were logit-normally distributed about some unknown mean mask initial filtration rate p_{avg} with a standard deviation σ_p , that is:

$$\text{logit}(p_{ij0}) \sim \text{Normal}(\text{logit}(p_{avg}), \sigma_p) \quad (16)$$

We then assumed that the logit of the filtration rate, $\text{logit}(p_{ijk})$, decreased after each decontamination by a quantity $d_{0k} + d_{ik}$, where d_{0k} is natural degradation during the k^{th} trial in the absence of

decontamination (i.e. the degradation rate in the control treatment, $i = 0$), and d_{ik} is the additional degrading effect of the k^{th} decontamination treatment of type $i > 0$. So for $k = 1, 2, 3$ and $i > 0$:

$$\text{logit}(p_{ijk}) = \text{logit}(p_{ij(k-1)}) - (d_{0k} + d_{ik}) + \varepsilon_{ijk} \quad (17)$$

where ε_{ijk} is a normally-distributed error term with an inferred standard deviation σ_ε :

$$\varepsilon_{ijk} \sim \text{Normal}(0, \sigma_\varepsilon) \quad (18)$$

And for the control $i = 0$:

$$\text{logit}(p_{0jk}) = \text{logit}(p_{0j(k-1)}) - d_{0k} + \varepsilon_{0jk} \quad (19)$$

Model prior distributions

We placed a weakly informative Half-Normal prior on the control degradation rate d_0 :

$$d_0 \sim \text{Half-Normal}(0, 0.5) \quad (20)$$

We placed a weakly informative Half-Normal prior on the non-control degradation rates d_i , $i > 0$:

$$d_i \sim \text{Half-Normal}(0.25, 0.5) \quad (21)$$

reflecting the conservative assumption that decontamination should degrade the mask at least somewhat.

We placed a Truncated Normal prior on the mean initial filtration p_{avg} :

$$p_{\text{avg}} \sim \text{TruncNormal}(0.995, 0.02) \quad (22)$$

The mode of 0.995 corresponds to the maximum measurable fit factor of 200. The standard deviation of 0.02 leaves it plausible that some masks could start near or below the minimum acceptable threshold fit factor of 100, which corresponds to a p of 0.99.

We placed weakly informative Half-Normal priors on the logit-space standard deviations σ_p , σ_e , and σ_o . σ_p reflects variation in individual masks' initial filtration about p_{avg} . σ_e reflects variation in mask's true degree of degradation between decontaminations about the expected decay, and σ_o reflects noise in the observation process.

$$\sigma_p, \sigma_e, \sigma_o \sim \text{Half-Normal}(0, 0.5) \quad (23)$$

We chose a standard deviation of 0.5 for the priors because a standard deviation of 1.5 (i.e. 3σ in the prior) in logit space corresponds to probability values being uniformly distributed between 0 and 1; we therefore wish to tell our model not to use larger standard deviations, as these squash all p_{ijk} to one of two modes, one at 0 and one at 1²³.

Markov Chain Monte Carlo Methods

For all Bayesian models, we drew posterior samples using Stan (Stan Core Team 2018), which implements a No-U-Turn Sampler (a form of Markov Chain Monte Carlo), via its R interface RStan. We ran four replicate chains from random initial conditions for 2000 iterations, with the first 1000 iterations as a warmup/adaptation period. We saved the final 1000 iterations from each chain, giving us a total of 4000 posterior samples. We assessed convergence by inspecting trace plots and examining R^2 and effective sample size (n_{eff}) statistics.

Supplemental table

Table S1. Effect of decontamination method on SARS-CoV-2 viability and N95 mask integrity.

Treatment	Material	half-life (min)			time to one thousandth (min)			time to one millionth (min)		
		median	2.5%	97.5%	median	2.5%	97.5%	median	2.5%	97.5%
Control	N95 mask	78	65.3	89.7	777	650	894	1.55e+03	1.3e+03	1.79e+03
	Steel	286	243	324	2.85e+03	2.42e+03	3.23e+03	5.7e+03	4.84e+03	6.45e+03
Ethanol	N95 mask	0.639	0.55	0.721	6.37	5.49	7.19	12.7	11	14.4
	Steel	1.06	0.888	1.23	10.6	8.85	12.2	21.2	17.7	24.5
Heat	N95 mask	4.64	3.87	5.41	46.3	38.5	53.9	92.6	77	108
	Steel	8.83	7.49	10.1	88	74.7	101	176	149	201
UV	N95 mask	6.26	5.31	7.15	62.4	52.9	71.2	125	106	142
	Steel	0.733	0.649	0.802	7.31	6.47	7.99	14.6	12.9	16
VHP	N95 mask	0.78	0.685	0.858	7.78	6.82	8.55	15.6	13.6	17.1
	Steel	0.765	0.669	0.843	7.63	6.67	8.4	15.3	13.3	16.8

Code and data availability

Code and data to reproduce the Bayesian estimation results and produce corresponding figures are archived online at OSF: and available on Github:

Acknowledgements

We would like to thank Madison Hebner, Julia Port, Kimberly Meade-White, Irene Offei Owusu, Victoria Avanzato and Lizzette Perez-Perez for excellent technical assistance. This research was supported by the Intramural Research Program of the National Institute of Allergy and Infectious Diseases (NIAID), National Institutes of Health (NIH). JOL-S and AG were supported by the Defense Advanced Research Projects Agency DARPA PREEMPT # D18AC00031 and the UCLA AIDS Institute and Charity Treks, and JOL-S was supported by the U.S. National Science Foundation (DEB-1557022), the Strategic Environmental Research and Development Program (SERDP, RC□2635) of the U.S. Department of Defense. Names of specific vendors, manufacturers, or products are included for public health and informational purposes; inclusion does not imply endorsement of the vendors, manufacturers, or products by the US Department of Health and Human Services.

Supplemental references

1. Ranney ML, Griffeth V, Jha AK. Critical Supply Shortages - The Need for Ventilators and Personal Protective Equipment during the Covid-19 Pandemic. *N Engl J Med* 2020.
2. Ong SWX, Tan YK, Chia PY, et al. Air, Surface Environmental, and Personal Protective Equipment Contamination by Severe Acute Respiratory Syndrome Coronavirus 2 (SARS-CoV-2) From a Symptomatic Patient. *JAMA* 2020.
3. van Doremalen N, Bushmaker T, Morris DH, et al. Aerosol and Surface Stability of SARS-CoV-2 as Compared with SARS-CoV-1. *N Engl J Med* 2020.
4. Decontamination and Reuse of Filtering Facepiece Respirators . 2020. (Accessed 4/5/2020, 2020, at <https://www.cdc.gov/coronavirus/2019-ncov/hcp/ppe-strategy/decontamination-reuse-respirators.html>.)
5. Final Report for the Bioquell Hydrogen Peroxide Vapor (HPV) Decontamination for Reuse of N95 Respirators. 2016. at <https://www.fda.gov/media/136386/download>.)
6. Fisher EM, Shaffer RE. A method to determine the available UV-C dose for the decontamination of filtering facepiece respirators. *J Appl Microbiol* 2011;110:287-95.
7. Heimbuch BK, Kinney K, Lumley AE, Harnish DA, Bergman M, Wander JD. Cleaning of filtering facepiece respirators contaminated with mucin and *Staphylococcus aureus*. *Am J Infect Control* 2014;42:265-70.
8. Heimbuch BK, Wallace WH, Kinney K, et al. A pandemic influenza preparedness study: use of energetic methods to decontaminate filtering facepiece respirators contaminated with H1N1 aerosols and droplets. *Am J Infect Control* 2011;39:e1-9.
9. Lin TH, Tang FC, Hung PC, Hua ZC, Lai CY. Relative survival of *Bacillus subtilis* spores loaded on filtering facepiece respirators after five decontamination methods. *Indoor Air* 2018.
10. Mills D, Harnish DA, Lawrence C, Sandoval-Powers M, Heimbuch BK. Ultraviolet germicidal irradiation of influenza-contaminated N95 filtering facepiece respirators. *Am J Infect Control* 2018;46:e49-e55.

11. Viscusi DJ, Bergman MS, Eimer BC, Shaffer RE. Evaluation of five decontamination methods for filtering facepiece respirators. *Ann Occup Hyg* 2009;53:815-27.
12. Avilash Cramer ET, Sherryl H Yu, Mitchell Galanek, Edward Lamere, Ju Li, Rajiv Gupta, Michael P Short. disposable N95 masks pass qualitative fit-test but have decreases filtration efficiency after cobalt-60 gamma irradiation. *MedRxiv*.
13. Chemical Disinfectants, Guideline for Disinfection and Sterilization in Healthcare Facilities. 2008. at <https://www.cdc.gov/infectioncontrol/guidelines/disinfection/disinfection-methods/chemical.html#Hydrogen>.)
14. Lin TH, Chen CC, Huang SH, Kuo CW, Lai CY, Lin WY. Filter quality of electret masks in filtering 14.6-594 nm aerosol particles: Effects of five decontamination methods. *PLoS One* 2017;12:e0186217.
15. N95 Respirators and Surgical Masks (Face Masks). 2020. (Accessed 4/5/2020, 2020, at <https://www.fda.gov/medical-devices/personal-protective-equipment-infection-control/n95-respirators-and-surgical-masks-face-masks>.)
16. Temporary Enforcement Guidance - Healthcare Respiratory Protection Annual Fit-Testing for N95 Filtering Facepieces During the COVID-19 Outbreak. 2020. at <https://www.osha.gov/memos/2020-03-14/temporary-enforcement-guidance-healthcare-respiratory-protection-annual-fit>.)
17. User Seal Check Procedures (Mandatory). 2020. (Accessed April 11, 2020, at <https://www.osha.gov/laws-regs/regulations/standardnumber/1910/1910.134AppB1>.)
18. Respirator Fit Testing [WWW Document]. U. S. Dep. Labo. 2012. at https://www.osha.gov/video/respiratory_protection/fittesting_transcript.html (accessed 4.10.20).)
19. Holshue ML, DeBolt C, Lindquist S, et al. First Case of 2019 Novel Coronavirus in the United States. *N Engl J Med* 2020.
20. van Doremalen N, Bushmaker T, Munster VJ. Stability of Middle East respiratory syndrome coronavirus (MERS-CoV) under different environmental conditions. *Euro Surveill* 2013;18.
21. Brownie C, Statt J, Bauman P, et al. Estimating viral titres in solutions with low viral loads. *Biologicals* 2011;39:224-30.
22. Gelman A. Bayesian data analysis. Third edition. ed. Boca Raton: CRC Press; 2014.
23. Northrup JM, Gerber BD. A comment on priors for Bayesian occupancy models. *PLoS One* 2018;13:e0192819.